

Review

# Hydrogen Bond and Other Lewis Acid–Lewis Base Interactions as Preliminary Stages of Chemical Reactions

Sławomir J. Grabowski <sup>1,2</sup> 

<sup>1</sup> Polimero eta Material Aurreratuak: Fisika, Kimika eta Teknologia, Kimika Fakultatea, Euskal Herriko Unibertsitatea UPV/EHU & Donostia International Physics Center (DIPC) PK 1072, 20080 Donostia, Euskadi, Spain; s.grabowski@ikerbasque.org; Tel.: +34-943-018-187

<sup>2</sup> IKERBASQUE, Basque Foundation for Science, 48011 Bilbao, Spain

Academic Editor: Ilya G. Shenderovich

Received: 23 September 2020; Accepted: 10 October 2020; Published: 13 October 2020



**Abstract:** Various Lewis acid–Lewis base interactions are discussed as initiating chemical reactions and processes. For example, the hydrogen bond is often a preliminary stage of the proton transfer process or the tetrel and pnictogen bonds lead sometimes to the  $S_N2$  reactions. There are numerous characteristics of interactions being first stages of reactions; one can observe a meaningful electron charge transfer from the Lewis base unit to the Lewis acid; such interactions possess at least partly covalent character, one can mention other features. The results of different methods and approaches that are applied in numerous studies to describe the character of interactions are presented here. These are, for example, the results of the Quantum Theory of Atoms in Molecules, of the decomposition of the energy of interaction or of the structure-correlation method.

**Keywords:** Lewis acid–Lewis base interactions; hydrogen bond; tetrel bond; pnictogen bond; triel bond; electron charge shifts

## 1. Introduction

It is well known that the hydrogen bond plays a crucial role in numerous chemical, physical and biological processes [1,2]. However, other interactions are also important in various processes, particularly biochemical ones [3,4]. It is worth mentioning that such terms as interaction and reaction are even used interchangeably sometimes since interactions often lead to corresponding reactions or at least they are initiative steps of chemical reactions. The aim of this study is to display dependencies between the latter phenomena. The interrelations between interactions and reactions as well as between them and other phenomena and processes, or reasons for the lack of such relations, were discussed in numerous studies, even in very early ones. For example, Lewis has described that “at the recent conference of the Faraday Society (July, 1923) all of those who participated seemed agreed that the average organic molecule is very little polarized, but there were some who believed that polarisation and indeed ionisation precede every reaction” [5].

More recent studies indicate an important role of electron charge shifts (related to the polarisation) in processes corresponding to interactions and then to chemical reactions. For example, Rauk has stated that “all reactions of organic compounds are treated within the framework of generalized Lewis acid - Lewis base theory, their reactivity being governed by the characteristics of the frontier orbitals of the two reactants. All compounds have occupied molecular orbitals and so can donate electrons, that is, act as bases in the Lewis sense. All compounds have empty molecular orbitals and so can accept electrons, that is, act as acids in the Lewis sense” [6].

It was also indicated that the term “noncovalent interactions” is not a proper one since it concerns hydrogen bond and halogen bond as well as other interactions that often possess characteristics of

covalent bonds [7]. The covalent character is often related to the occurrence of polarization and charge transfer processes [8,9]. On the other hand, for very weak interactions ruled mainly by dispersion forces, the electron charge shifts are negligible, if there are any, also electrostatic interactions are not important there. This is why the term Lewis acid–Lewis base interactions seems to be the proper one since it is related to those interactions where the electron charge shifts occur between Lewis acid and Lewis base units. It seems also that this term excludes very weak interactions, as those that occur between methane molecules, for example, where dispersion forces are the most important ones and where it is difficult to indicate the Lewis acid and Lewis base centres [7].

Kaplan has concluded in his monograph that “intermolecular interactions are involved in the formation of complicated chemical complexes, such as charge-transfer and hydrogen-bond complexes. Study of the mechanism of elementary chemical reactions is impossible without knowledge of the exchange processes between the translational and electron-vibration energies, which depend on the interaction of particles under collisions. Knowledge of the potential surface, characterizing the mutual trajectories of the reactants, is necessary to obtain the rates of chemical reactions” [10].

This is why the aim of this review is to point out relationships between interactions and reactions since the former phenomena may lead to the latter ones thus they initiate numerous structural changes and electron charge redistributions in species being in contact. This is of particular interest, which characteristics possess interactions that lead to chemical reactions. It was discussed in one of recent reviews that the stronger electrostatic interactions lead to the stronger Pauli repulsion that implies the greater electron charge shifts, mainly from the Lewis base unit to the Lewis acid; these phenomena may lead to the chemical reaction [11]. In this review, few types of interactions are discussed and it is analysed which conditions should be fulfilled for them that they lead to chemical reactions.

## 2. The Hydrogen Bond as a Preliminary Stage of the Proton Transfer Process

It has been described in early studies that a fragment of a crystal structure may be treated as “a frozen stage” of a considered chemical reaction. The related fragments that differ by geometry and that are taken from various crystal structures may correspond to the analysed chemical reaction since they reflect structural changes accompanying this reaction [12–14]. This approach is known as the structure-correlation method. It was applied to analyse different reactions such as the nucleophilic addition to a carbonyl group, nucleophilic substitution at tetrahedral coordinated atoms ( $S_N1$  and  $S_N2$  reactions); electrocyclic ring closure of polyenes and other chemical processes [12–15].

It is important that the proton transfer, PT, process related to the hydrogen bond, HB, may be also discussed in terms of the structure-correlation method. For example, PT in  $O-H\cdots O$  hydrogen bonds was analysed since  $-C=O\cdots H-O-C-$  fragments taken from different crystal structures were compared to reconstruct the corresponding reaction path [9,11,16]. For these analyses, the high-precision neutron diffraction geometries were taken from the Cambridge Structural Database, CSD [17,18]. The recent CSD release (CSD updates up to May 2020) was applied here to search the above-mentioned  $-C=O\cdots H-O-C-$  fragment with the following search criteria; accurate crystal structures with  $e.s.d.'s \leq 0.005 \text{ \AA}$ ,  $R \leq 7.5\%$ , error free structures, without disorder, no polymers and no powder diffraction results. Only neutron diffraction results were taken into account here since they are characterised by precisely determined positions of H-atoms [19] in contrast to the X-ray results, where the refinement of crystal structures is usually based on the spherical approximation of the atomic electron densities that results in the spherical symmetry of atomic scattering factors [20]. One may say that the sample of fragments described above and corresponding to different crystal structures of organic and organometallic compounds may reflect the reaction path of the following PT process;  $-C=O\cdots H-O-C- \leftrightarrow -C-O-H\cdots O=C-$ . In some of structures H-atom is situated in the mid-point of the  $O\cdots O$  distance or near to this point therefore  $-C=O\cdots H^+\cdots O=C-$  fragments are also included in the sample. The search has led to a finding of 56 geometrical fragments corresponding to the above-mentioned PT process. The similar search with the same criteria for accuracy of results was performed for the similar fragments where the

H-atom is replaced by the deuterium, i.e., the  $\text{-C=O}\cdots\text{D-O-C-}$  fragments; in this case only four structures were found.

Figure 1 presents the PT reaction path based on two above described CSD searches; this is the relationship between the  $\Delta r$  parameter and the  $\text{O}\cdots\text{O}$  distance. The same relationships were discussed before [9,11,16] but they were based on earlier CSD updates. The  $\Delta r$  parameter is the distance of the H-atom of the  $\text{O-H}\cdots\text{O}$  bridge from the  $\text{O}\cdots\text{O}$  mid-point. For the linear  $\text{O-H(D)}\cdots\text{O}$  systems the  $\text{O}\cdots\text{O}$  distance may be expressed as the  $r_{\text{O-H}} + r_{\text{H}\cdots\text{O}}$  sum while the  $\Delta r$  parameter as the  $(r_{\text{H}\cdots\text{O}} - r_{\text{O-H}})/2$  term. The  $r_{\text{O-H}}$  and  $r_{\text{H}\cdots\text{O}}$  values correspond to the O-H bond length and the H...O distance, respectively. The points of Figure 1, which correspond to fragments of crystal structures, may be considered as positions of the proton in PT process. The results of this figure are symmetrised around  $\Delta r = 0$ ; this symmetrisation corresponds to the equivalency of systems during PT reaction because the homonuclear  $\text{O-H}\cdots\text{O}$  hydrogen bond is discussed here. The “points” in the middle of  $\text{O}\cdots\text{O}$  distance may be considered as the transition state of the proton transfer reaction. These are strongly elongated O-H bonds and they are observed for the  $\text{O}\cdots\text{O}$  distances amounting about  $\sim 2.4\text{--}2.5$  Å. For long  $\text{O}\cdots\text{O}$  distances the H-atoms are located far from their mid-points, they are situated close to one of oxygen centres rather.

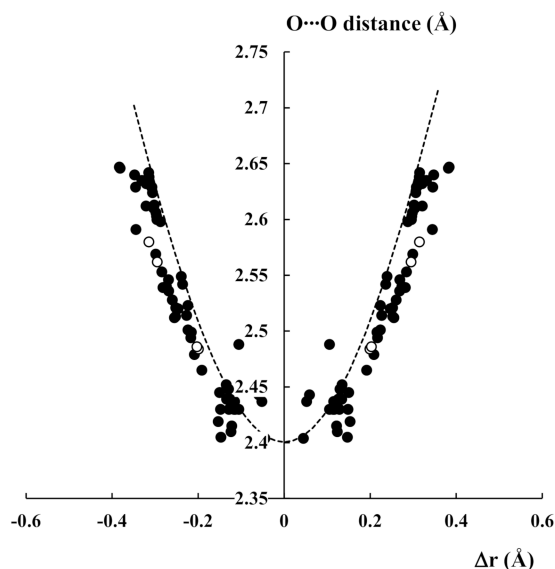


**Figure 1.** The dependence between the  $\Delta r$  (Å) - the displacement of the proton (or deuter) position from the  $\text{O}\cdots\text{O}$  mid-point and the  $\text{O}\cdots\text{O}$  distance (Å), for the  $\text{O-H}\cdots\text{O}$  systems (black circles) and the  $\text{O-D}\cdots\text{O}$  ones (white circles). The broken line corresponds to the bond number conservation rule (Equation (1)).

The broken line of Figure 1 corresponds to the relationship expressing the bond order (number) conservation rule (Equation (1)) [12,13,21].

$$\exp\left(\frac{\Delta r_i}{c}\right) + \exp\left(\frac{\Delta r_j}{c}\right) = 1 \quad (1)$$

The  $\Delta r_i$  and  $\Delta r_j$  terms in the above equation correspond to the  $(r_0 - r_{\text{O-H}})$  and  $(r_0 - r_{\text{H}\cdots\text{O}})$  differences;  $r_0$  is the typical single O-H bond length not perturbed by any interaction. The bond length of water in the gas phase equal to  $0.957$  Å was chosen here and in other studies [9]. The exponential terms of Equation (1),  $\exp(\Delta r_i/c)$ , may be treated as the definition of the bond order. However, other names for this term as well as for similar expressions are often applied in various studies; the bond valence [21] or the bond number [22], for example. The constant  $c$  for the  $\text{O-H}\cdots\text{O}$  hydrogen bonds is determined from the above exponential expression assuming that for the  $\text{O-H}\cdots\text{O}$  linear system with the H-atom

located in the O...O mid-point, and the O...O distance of 2.4 Å, two equivalent H...O distances possess the bond order equal to 0.5; in other words;  $c = (0.957 - 1.2)/\ln(0.5)$ .

The bond order and the bond order conservation rule ideas for the O-H...O hydrogen bonds may be described in the following way. For the single O-H bond in the gas phase, the bond order is equal to unity. If this bond is involved in the hydrogen bond thus it is elongated and its bond order decreases. However, this decrease is compensated by the H...O contact. Hence the sum of bond orders (Equation (1)) of the O-H bond and the H...O contact is equal to unity. The greater is the O-H bond elongation for the stronger hydrogen bond thus the greater is the bond order of the H...O contact that is shorter accordingly; the latter is also accompanied by the decrease of the O...O distance (Figure 1). The extreme cases of very short O...O distances with the H-atom location at the O...O mid-point for very strong hydrogen bonds correspond to the transition states of the proton transfer reaction.

One can see that the broken line of Figure 1 that was derived from the bond order conservation rule is only approximately in agreement with the neutron diffraction results. Similar disagreement concerning the relationship between the O-H bond length and the H...O distance was explained by the influence of electrostatic forces that are not properly included in the bond order conservation concept [23]. Hence the corrected reference single O-H bond length of 0.925 Å was proposed to take into account the electrostatic contribution and to have better agreement between experimental results and theoretical evaluations [23]. Figure 1 contains also the O-D...O systems; it is pointed out in several studies that the deuteration of the O-H...O systems results in shortening of the O-D bond and lengthening of the O...O and D...O distances in comparison with their non-deuterated counterparts; it is known as the Ubbelohde effect [24]. Figure 1 shows that the deuterated O-D...O systems are approximately in agreement with the broken curve derived from Equation (1). One may conclude that the reaction path presented in Figure 1 shows that the hydrogen bond, especially for the strong O-H...O interactions, may be treated as the initial stage of PT process.

It is worth mentioning that similar relationships to this one presented in Figure 1 were analysed for other hydrogen bonded systems. For example, it was found that the dependence between  $q_1$  and  $q_2$  parameters for the N-H...N hydrogen bond geometries taken from experimental NMR and crystal structures' results is in agreement with the bond order conservation rule expressed by an equation similar to that one presented above here (Equation (1)) [25]. The  $q_1$  and  $q_2$  parameters are equal to  $(r_{H...N} - r_{N-H})/2$  and  $r_{H...N} + r_{N-H}$ , respectively;  $r_{H...N}$  is the H...N distance and  $r_{N-H}$  is the N-H bond length in the N-H...N system.

In another study the proton bound water dimer,  $H_5O_2^+$  (Zundel cation) was discussed [26]. The relationships between molecular structures of this cation and the  $^1H$ -NMR chemical shifts were presented; low-temperature neutron diffraction results were used for these relationships. The dependence between  $q_1 = (r_{H...O} - r_{O-H})/2$  and  $q_2 = r_{H...O} + r_{O-H}$  parameters that is very similar to that one presented in Figure 1 has been also discussed [26]. The chemical shifts and other NMR parameters were also analysed for the N-H...N [25,27], F-H...N [28] and F-H...F<sup>-</sup> [28] hydrogen bonded systems. The bond order conservation rule [9,12] was compared there with the experimental results and with the theoretical calculations [25,27,28].

One can see that the geometries of hydrogen bonded systems represent various stages of the proton transfer reaction. It is discussed above here for different types of hydrogen bonds. As a consequence, the question arises, what are the characteristics of hydrogen bonds that may be treated as the initial stages of the PT process? It was discussed in earlier studies [9,11,29] that the strong hydrogen bonds may lead to the proton transfer reactions. It is worth recalling here effects that accompany the A-H...B hydrogen bond formation. It is the Lewis acid–Lewis base interaction thus the noticeable electron charge shift from the base unit to the acidic one occurs here [7,11]. This is connected with the  $n_B \rightarrow \sigma_{AH}^*$  orbital-orbital interaction [8], where  $n_B$  is the lone electron pair orbital of the B-centre while  $\sigma_{AH}^*$  is the antibonding orbital of the A-H  $\sigma$ -bond. If we exclude from our discussion the blue shift hydrogen bonds [30] which do not lead to the PT process rather thus the hydrogen bond formation is connected with the increase of the polarization of the A-H bond, its elongation and consequently

with its weakening. In extreme cases of the strong hydrogen bonds possessing covalent or at least partly covalent character [9] the PT reaction occurs. The terms resulting from the decomposition of the energy of interaction and related to the electron charge shifts are described as those expressing the covalency. The following terms occur in different decomposition schemes: charge transfer, polarization, delocalization or induction term. The name of term depends on the decomposition scheme applied. The interaction energy contributions differ by physical meaning in different schemes although they similarly express processes related to the electron charge shifts.

The covalent character may be also detected by the Quantum Theory of Atoms in Molecules (QTAIM) approach [31,32]. The value of the electron density at the H...B bond critical point (BCP),  $\rho_{\text{BCP}}$ , of the order of 0.1 u and more, and the negative Laplacian of this electron density,  $\nabla^2\rho_{\text{BCP}}$ , inform of the covalent character of the hydrogen bond. However, it is assumed in numerous studies that even for  $\nabla^2\rho_{\text{BCP}} > 0$ , the negative value of the total electron energy density at BCP,  $H_{\text{BCP}}$ , shows the partly covalent character of interaction [9,33–36].

Figure 2 presents the relationship between the hydrogen...Lewis base distance and the  $H_{\text{BCP}}$  value at the corresponding BCP, for the sample of hydrogen bonds analysed in earlier study [37]. These results are based on the MP2/6-311++G(d,p) calculations. The following complexes linked by hydrogen bonds were discussed there. The complexes connected by charge assisted hydrogen bonds (CAHBs):  $(\text{FHF})^-$ ,  $\text{H}_2\text{O}\cdots\text{H}_3\text{O}^+$ ,  $\text{H}_3\text{O}^+\cdots\text{HCN}$ ,  $\text{OH}^-\cdots\text{H}_2\text{O}$ ,  $\text{NH}_3\cdots\text{NH}_4^+$ ,  $\text{C}_5\text{H}_5^-\cdots\text{HF}$  and  $\text{C}_5\text{H}_5^-\cdots\text{C}_2\text{H}_2$ . The complexes with  $\pi$ -electrons acting as the acceptor of proton, these are two latter CAHB systems as well as the following species;  $\text{C}_2\text{H}_2\cdots\text{HF}$ ,  $\text{C}_2\text{H}_4\cdots\text{HF}$ ,  $\text{C}_6\text{H}_6\cdots\text{HF}$ ,  $(\text{C}_2\text{H}_2)_2$  (T-shaped dimer),  $\text{C}_2\text{H}_4\cdots\text{C}_2\text{H}_2$ ,  $\text{C}_6\text{H}_6\cdots\text{C}_2\text{H}_2$ ,  $\text{C}_6\text{H}_6\cdots\text{CH}_4$ ,  $\text{C}_6\text{H}_6\cdots\text{CHCl}_3$ ,  $\text{C}_2\text{H}_2\cdots\text{CH}_4$  and  $\text{C}_2\text{H}_2\cdots\text{CHCl}_3$ . There is the sub-sample of complexes linked by the C-H...B hydrogen bonds:  $\text{F}_3\text{CH}\cdots\text{NCCH}_3$ ,  $\text{H}_3\text{CH}\cdots\text{NCCH}_3$ ,  $\text{HCCH}\cdots\text{NCCH}_3$ ,  $\text{F}_3\text{CH}\cdots\text{OCH}_2$ ,  $\text{H}_3\text{CH}\cdots\text{OCH}_2$ ,  $\text{HCCH}\cdots\text{OCH}_2$ ,  $\text{H}_3\text{CH}\cdots\text{SH}_2$ ,  $\text{HCCH}\cdots\text{SH}_2$  and  $\text{HCCH}\cdots\text{S}(\text{CH}_3)_2$ . The other hydrogen bonds analysed in the above-mentioned study [37] may be classified as moderate or strong ones, these are interactions in the following complexes;  $(\text{C}_6\text{H}_5\text{COOH})_2$ ,  $(\text{CH}_3\text{COOH})_2$ ,  $(\text{HCOOH})_2$ ,  $(\text{HCONH})_2$ ,  $(\text{HCSNH})_2$ ,  $(\text{H}_2\text{O})_2$  (trans-linear dimer),  $\text{H}_2\text{O}\cdots\text{HF}$  and  $\text{H}_2\text{CO}\cdots\text{HF}$ . The hydrogen bonds are divided into three groups in Figure 2, C-H... $\pi$  (open circles, the  $\text{C}_5\text{H}_5^-\cdots\text{HF}$  complex with the F-H proton donating bond is also included there), C-H...B (black squares) and remaining ones, among them CAHB systems (black circles). The hydrogen...Lewis base distance is understood here in the following way: it is the H...B distance for the 3c-4e (three centre-four electron [8]) A-H...B hydrogen bonds. For the C-H... $\pi$  interactions this is the distance between the H-atom of Lewis acid unit and the carbon atom or the bond critical point of CC bond of the Lewis base [37]. The latter depends on the kind of the bond path characterizing the intermolecular link [37]. Figure 2 shows that for stronger interactions characterised by shorter distances between Lewis acid-base units the covalent character is revealed that is expressed by the negative  $H_{\text{BCP}}$  values, the corresponding systems may be treated as the potentially preliminary stages of PT processes. The weaker hydrogen bonds are characterised by longer distances between these units, these are mainly the C-H... $\pi$  and C-H...B systems.

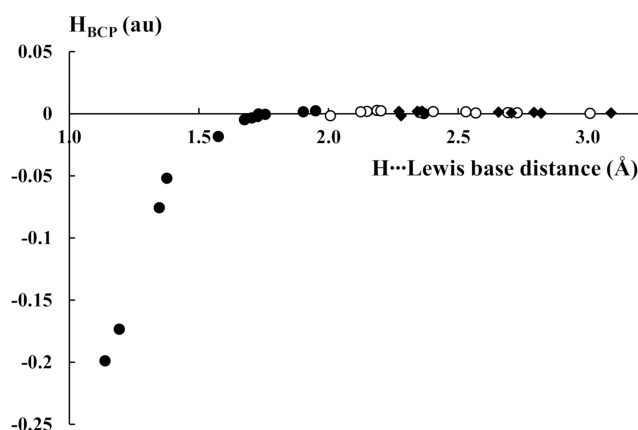


**Figure 2.** The dependence between the H...Lewis base distance (between H-atom of the proton donor and the centre of Lewis base unit, in Å) and the total electron energy density at BCP,  $H_{BCP}$  for hydrogen bonded systems. The Lewis base centre is an atom for 3c–4e A–H...B hydrogen bonds (black squares for C–H...B hydrogen bonds and black circles for other 3c–4e systems) and it is BCP of CC bond or C-atom in Lewis base unit for the A–H... $\pi$  hydrogen bonds (while circles).

### 3. The Case of Halogen Bonds

There are several various interactions that are treated in numerous studies as the hydrogen bond counterparts, particularly it concerns so-called  $\sigma$ -hole and  $\pi$ -hole bonds [38–42]. The  $\sigma$ -hole is a region of electron charge depletion at a centre considered approximately in the direction from an atom bonded to this centre, in the elongation of this bond [38,39]. On the other hand, the  $\pi$ -hole concerns a centre in a planar molecule or a planar molecular fragment [41,42], the triel centres such as boron one in trihalides and trihydrides are examples of such a situation [43,44]. The electron charge depletion at the  $\sigma$ -holes and  $\pi$ -holes often leads to the positive electrostatic potential, EP, at these regions; hence they often act as the Lewis acid centres.

The halogen bond, XB, is a case of an interaction where the  $\sigma$ -hole at halogen centre, X (F, Cl, Br, I or At) i.e., the Lewis acid site, interacts with the Lewis base centre [38,39]. This is why this interaction is often considered as the hydrogen bond counterpart, in numerous studies the comparison of these interactions is performed [11,40,45–47]. However, there is the question if XB, similarly as the hydrogen bond, may be considered as a preliminary stage of the chemical reaction. The PT process follows sometimes the hydrogen bond formation. Does a similar transfer of a halogen atom occur? Let us discuss shortly studies, particularly the recent ones, on the entities with halonium cation that links two Lewis base centres. The latter topic is revealed in recent studies by two challenges. The first one concerns finding of Lewis base–halonium ion–Lewis base arrangements with asymmetrically located halonium cation [48]. They are designated later here as  $[LbXLb]^+$ , where in further discussions Lb is replaced by the specific atomic centre while X marks the halogen. The second challenge concerns finding of the  $[LbXLb]^+$  arrangement with fluorine, X = F, situated between the Lewis base sides since rather such systems with heavier halogens are known [49]. As concerns the latter challenge, the generation of a symmetrical fluoronium ion in solution was discussed, its existence was evidenced indirectly [50]. These experimental studies were supported by the calculations performed at various levels, all levels applied confirmed this ion existence, for example, the B3LYP/6-311++G(d,p) results show equal F...C distances amounting 1.6 Å in the  $[CFC]^+$  arrangement [50]. It was proved in numerous earlier and recent studies that the heavier halogen atom (Cl, Br, I) may be engaged in the hypervalent link in solution possessing formally positive charge. Such a link was usually doubted for the fluorine centre; the studies of Lectka and co-workers discussed here [49,50] are related to this challenge. However, it was evidenced only indirectly the occurrence of the fluoronium ion as a short-lived reaction intermediate [50]. It was discussed also that this ion is formed in a solvolysis process from a precursor molecule probably according to the  $S_N1$  reaction through the fluorine centre [50,51]. The crystal

structure of the fluoronium ion precursor was determined [50]; the structure of this ion taken from the Cambridge Structural Database, CSD [17,18] is presented in Figure 3. The direct observation of the similar symmetrical  $[\text{CFC}]^+$  ion was described recently [49], this is a stable species in solution and it was characterised by  $^{19}\text{F}$ ,  $^1\text{H}$ , and  $^{13}\text{C}$  NMR.

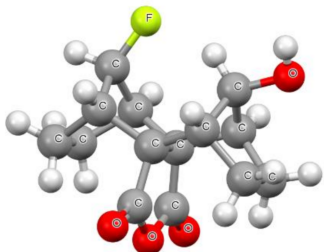


**Figure 3.** The fluoronium ion precursor from the crystal structure [50], BEXNOJ refcode.

Another challenge announced here concerns asymmetric  $[\text{NXN}]^+$  systems since the symmetrical systems containing the halogen, X, are known rather from various studies [48]. For example, the experimental NMR spectroscopic and crystal structure studies as well as the theoretical calculations were performed recently on the systems containing halogen cation as well as other cations between nitrogen centres, i.e., the  $[\text{NZN}]^+$  systems where  $\text{Z}^+ = \text{H}^+, \text{Li}^+, \text{Na}^+, \text{F}^+, \text{Cl}^+, \text{Br}^+, \text{I}^+, \text{Ag}^+$  and  $\text{Au}^+$  [52]. Two series, one of bis(pyridine) entities and the second one containing the (1,2-bis(pyridin-2-ylethynyl)benzene) structure were considered [52]. In all cases the symmetrical arrangements are observed, only for  $\text{Z}^+ = \text{H}^+$  and  $\text{F}^+$  the asymmetric systems occur; this concerns both above-mentioned series. However, in a case of the fluorine species there is no experimental confirmation of such asymmetry, only theoretical calculations reveal such arrangements. Figures 4 and 5 show fragments of bis(pyridine) crystal structures. In two cases (Figure 4); silver [53] and iodine [53] cations are located in the centre of the  $[\text{NAgN}]^+$  and  $[\text{NIN}]^+$  systems, respectively. In a case of the bis(pyridine)proton structure the asymmetric  $[\text{NHN}]^+$  arrangements are observed [54] (see Figure 5).

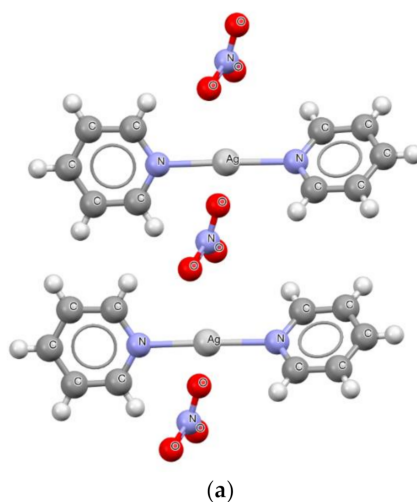


**Figure 4.** Cont.

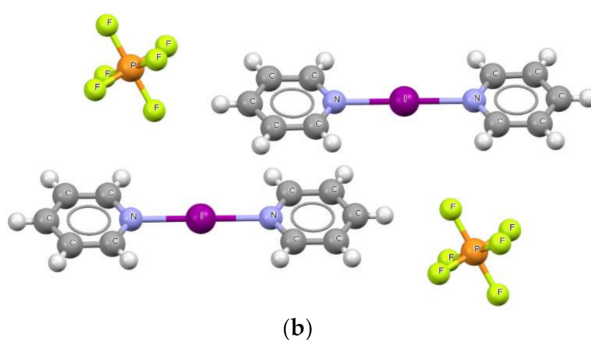


**Figure 4.** The fragment of the crystal structure of bis(pyridine)-silver(i) nitrate monohydrate, AGPYNO02 refcode (a) and di(pyridin-1-yl)iodonium hexafluorophosphate, CICQIQ03 refcode (b), reference [53].

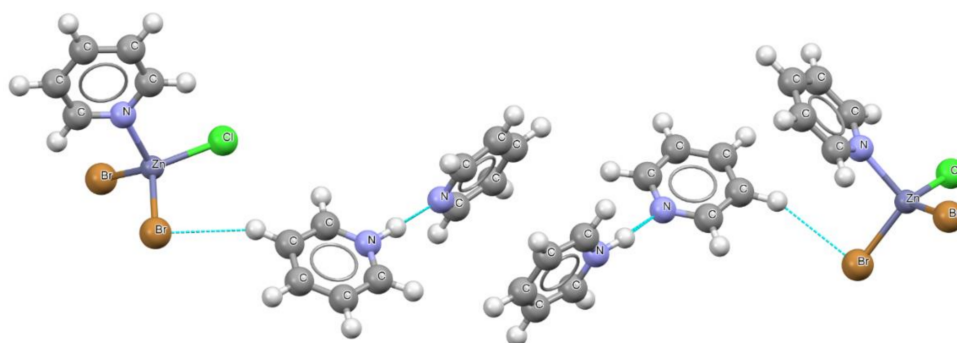


**Figure 5.** The fragment of the crystal structure of pyridinium dibromo-chloro-pyridine-zinc(ii) pyridine solvate, PYCBZN01 refcode, reference [54].

It is worth mentioning that the potential energy curves were analysed theoretically for the bis(pyridine) series of complexes [52], the displacement of the  $Z^+$  cation from the N...N mid-point was plotted versus the electronic energy of the system. The single well potential energy curve is observed for all systems except of  $Z^+ = H^+, F^+$  where the double minimum symmetrical curve occurs [52]. Since the similar situation occurs for the series of 1,2-bis(pyridin-2-ylethynyl)benzene structures thus one can expect that the potential energy curve shape depends on the cation. However, this shape is a result of numerous factors; not only a kind of a cation. It depends on the type of a complex, the environment that results from the arrangement of molecules in crystals or from the type of solvent in liquids. For example, the first asymmetric linear silver complexes and the first asymmetric halonium complexes characterised by the  $[NAgN]^+$  and  $[NIN]^+$  arrangements, respectively, were analysed and they were confirmed by  $^1H$  and  $^1H-^{15}N$  HMBC NMR spectroscopy, and by X-ray diffraction results in crystals [55]. Thus one may expect that the halonium ion transfer and the transfer of other cations as  $Ag^+$ , for example, is possible for some systems. It is worth to mention that Zundel compared the hydrogen bond with analogues interactions where the proton is replaced by the lithium, sodium or potassium cations; the transfers similar to the proton transfer were analysed [56].

Let us compare systems containing  $Z^+$  cations that were discussed above with the hydrogen bonds. The examples presented earlier here indicate the asymmetric position of proton in  $[NHN]^+$  arrangement for both 1,2-bis(pyridin-2-ylethynyl)benzene and bis(pyridine) structures. It seems that the asymmetry of the H-atom position results, at least partly, from the asymmetry of environment in crystals. In another crystal structure containing protonated homodimer of pyridine, i.e., pyridinium tetrakis(3,5-bis(trifluoromethyl)phenyl)borate pyridine solvate, the asymmetry of the  $[NHN]^+$  arrangement is also observed; however the asymmetric  $[NHN]^+$  bridges occur also in solution [57]. The NMR signals in solution show the fast reversible proton transfer. All results concerning crystal as well as solution indicate the asymmetry of the  $[NHN]^+$  contact, in spite the

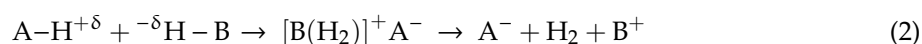


N-H...N hydrogen bond is very strong and covalent in nature and the weak anion coordination is observed. Other strong N-H...N hydrogen bonds in derivatives of proton-bound homodimer of pyridine were analysed in solution and it was also found they are asymmetric in spite of these being very strong interactions [58].

It is worth to note however that hydrogen bonds characterised by a single symmetrical minimum of potential energy curve are also well known. The [FHF]<sup>−</sup> anion is an example, the symmetrical species is known in the gas phase [59] although in crystal structure this anion is disturbed by packing forces since the movement of proton from the central position is often observed [60]. Similarly, the OH...O hydrogen bonds were analysed as it was discussed which conditions have to be fulfilled for the central position of proton [61]. Figure 1 presented earlier here shows geometries of numerous OH...O systems, the asymmetric ones as well as those where the proton is very close to the O...O mid-point. Various studies on hydrogen bonds, and particularly on the O-H...O systems indicate the complex character of PT process [62], for example, the potential barrier height should be taken into account in the analysis of this process. The same probably concerns the transfer of other cations, among them of halonium ones. There is no sufficient experimental and theoretical results however, and there is room for more extended investigations in this matter.

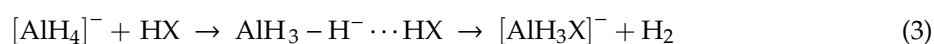
#### 4. The Dihydrogen Bond as a Stage of the Molecular Hydrogen Uptake

The dihydrogen bond, DHB, is a special type of the hydrogen bond where the Lewis base centre is the negatively charged hydrogen atom [63–65]. In other words, it is the link between hydrogen atoms of the opposite charge, H<sup>+δ</sup>...<sup>−δ</sup>H. The question arises if the proton transfer process A-H...B ⇌ A<sup>−</sup>...<sup>+</sup>H-B known for the A-H...B hydrogen bonded systems [62] occurs for dihydrogen bonds. This is discussed in detail in the monograph of Bakhmutov where numerous studies related to this topic are discussed [65]. It was generalised that the protonation of the hydride species characterised by the negatively charged hydrogen centre may be reversible or not, the latter phenomenon is connected with the molecular hydrogen elimination that may be expressed by the following transformations.



It is worth mentioning that the B centre connected with the hydric hydrogen is most often the transition metal, the numerous moieties containing molecular hydrogen attached to the transition metal centre are known, such systems often occur in crystal structures [66,67]. The model F-H<sup>+δ</sup>...<sup>−δ</sup>H-Li complex corresponding to the phenomena expressed by Equation (2) was analysed theoretically early at the HF/6-31G(d,p) level [68]. It was found that the presence of the external electric field may lead to the formation and elimination of the molecular hydrogen since there are the following products; F<sup>−</sup> + H<sub>2</sub> + Li<sup>+</sup>, of the proton transfer reaction. The reverse process is observed for the system containing dihydrogen molecule inserted between Lewis acid and Lewis base units, H<sub>3</sub>B...H<sub>2</sub>...NH<sub>3</sub> since the DHB system is formed in the external electric field; H<sub>3</sub>B<sup>−</sup>-H...H<sup>+</sup>NH<sub>3</sub> [68]. Bakhmutov, in his monograph [65], gives numerous examples of PT process in DHBs systems. The PT reaction and the dihydrogen elimination were discussed in the X-ray crystal structure of N-[2-(6-aminopyridyl)]acetamide cyanoborohydride [69], the solid state transformation from the dihydrogen bonded LiBH<sub>4</sub>-triethanolamine system to the covalent bonded material was described in another study [70].

There is an early example of the theoretical study [71] where the following reaction that leads to the molecular hydrogen uptake through the dihydrogen bond formation and next the proton transfer was analysed for a series of complexes of the AlH<sub>4</sub><sup>−</sup> anion.



The MP2/6-311++G(d,p) calculations were performed for this process (Equation (3)) with the HF, HCl, and H<sub>2</sub>O species acting as the proton donors. The transition states of the process of transformation

from the DHB systems to the products containing dihydrogen molecule were also calculated indicating that the PT reactions are energetically possible here, for example the potential barrier height for the  $\text{AlH}_3\text{-H}^- \cdots \text{HCl} \rightarrow [\text{AlH}_3\text{Cl}]^- + \text{H}_2$  reaction is equal to 6.7 kcal/mol.

In one of more recent studies [72] the reverse process of the molecular hydrogen cleavage at the metal centre that leads to the dihydrogen bonded complex formation was analysed;  $\text{FM} + \text{H}_2 \rightarrow \text{FH} \cdots \text{HM}$  ( $\text{M} = \text{Cu}, \text{Ag}, \text{Au}$ ). The calculations were performed with the use of the aug-cc-pVQZ basis set (aug-cc-pVQZ-PP for metal atoms) and the following methods, MP2, CCSD(T) and CASSCF/CASPT2. The systems with dihydrogen molecule attached to the metal centre correspond to global minima, while the dihydrogen bonded complexes are characterised by higher energies (local energetic minima). Only for complexes containing the gold centre the DHB system is lower in energy than the system with the  $\text{H}_2$  molecule for CASSCF/CASPT2 and CCSD(T) calculations. For example, for the CCSD(T)/aug-cc-pVQZ(aug-cc-pVQZ-PP) level of calculations for the  $\text{FAu} + \text{H}_2 \rightarrow \text{FH} \cdots \text{HAu}$  reaction the potential barrier height amounts 30.9 kcal/mol and the products of reaction are lower in energy than reactants by 1.5 kcal/mol.

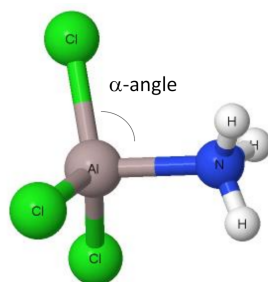
## 5. The Change of Trigonal Planar Triel Configuration into the Tetrahedral One—Triel Bonds

The triel bond is an interaction between the 13th group element acting as the Lewis acid centre and the electron-rich region of another or the same species [43,44,73]. It is worth to note that the acidic properties of triel atoms are related to the so-called  $\pi$ -holes [41,42] that are regions in planar molecules or in planar fragments of molecules at centres characterised by the depletion of the electron charge. For example, the trivalent triel atoms in trihydrides and trihalides possess formally empty p-orbital situated perpendicularly to the planes of molecules and being capable to act as the electron acceptor; numerous early [74–77] and more recent studies [43,44,73] related to interactions of the above-mentioned species with Lewis base units are known. The special attention should be paid to the studies of Phillips and co-workers who analysed such complexes from the theoretical and experimental points of view since the high level ab initio calculations were performed as well as the corresponding crystal structures were discussed [78–82]; particularly the potential energy as a function of the distance between the Lewis acid-base units was described [78]. It was found that the double local minimum occurs for some of complexes, deeper one corresponding to shorter distances and the flat, shallow energy minimum for the longer distances. The former minimum corresponds to strong and partly covalent interactions while the latter local minimum to weak interactions characterised mostly by dispersion forces. These findings are in line with other more recent studies [73,83].

It is worth to mention that for the triel bonds, similarly as for the hydrogen bonds, different sub-classes of interactions exist [84]. There are triel bonds with the one-centre electron donor,  $\text{A-T} \cdots \text{B}$  (where T is the triel atom, B is the electron donor and A is any atom connected with the triel centre), the interactions with  $\pi$ -electrons acting as the electron donor,  $\text{A-T} \cdots \pi$  where the alkenes and alkynes were considered as the Lewis base units [85,86] as well as benzene entity [87]. Another sub-class concerns links where the  $\sigma$ -bonds' electrons play a role of the electron donors,  $\text{A-T} \cdots \sigma$  interactions; the complexes of molecular hydrogen acting as the Lewis base unit with the boron trihydride and boron trihalides were analysed in early study [85] and more recently the complexes of molecular hydrogen with boron and aluminium trihydrides and trifluorides were analysed theoretically [88]. Finally, one can mention intramolecular and bifurcated triel bonds that occur in the crystal structures [89]. It is well known that such types of hydrogen bonds are common in crystals [1,2,90].

The most interesting is which structural changes follow the formation of triel bonds? For example, the trivalent triel species described shortly above here change their planar structure if they interact with Lewis bases. The stronger interactions result in greater changes in the triel species geometry; in a case of extremely strong interactions, for example with anions, the triel centre conformation becomes to be close to tetrahedral structures. Even it acquires an ideal  $T_d$  symmetry like in the  $\text{BF}_4^-$  anions which occur very often in crystal structures [91]. Scheme 1 presents an example of the  $\text{AlCl}_3 \cdots \text{NH}_3$  complex linked by the  $\text{Al} \cdots \text{N}$  triel bond. The  $\alpha$ -angle which may be treated as the parameter of the

deformation resulting from complexation is defined in this scheme. It is the angle between the Al...N line corresponding to the triel bond and one of the Al-Cl bonds. The angle parameter may be applied to other simple triel species complexes that informs the Lewis acid unit deformation resulting from the triel bond formation. This angle is equal to  $90^\circ$  if the interaction is very weak and the molecular deformations are not detected, it means that the triel Lewis acid species is still planar, or at least it is close to planarity. The increase of the  $\alpha$ -angle is observed with the increase of the strength of interaction, for the  $\text{BF}_4^-$  anion being the result of the  $\text{BF}_3 \dots \text{F}^-$  interaction it amounts  $109.5^\circ$  like for methane and other species possessing  $T_d$  symmetry.



**Scheme 1.** The  $\text{AlCl}_3 \dots \text{NH}_3$  complex linked by the Al...N triel bond.

Figure 6 presents the relationship between the triel centre - Lewis base centre distance and the  $\alpha$ -angle for simple complexes of boron and aluminium trihydrides and trichlorides. This dependence is based on the MP2/aug-cc-pVTZ results that come from one of recent studies [73]. The following Lewis base units were taken into account there; HCN,  $\text{NH}_3$ ,  $\text{N}_2$  and  $\text{Cl}^-$ . In such a way three sub-classes of complexes are presented in Figure 6; the ionic species being complexes with chloride anion and the remaining complexes are divided into two groups: complexes of aluminium Lewis acid units and complexes of boron compounds. The excellent linear correlation is observed for the neutral complexes of aluminium. For the remaining complexes, only tendency is observed that for stronger interactions (shorter Lewis acid-base distances) the greater  $\alpha$ -angle occurs. In two cases of ionic systems,  $\text{BCl}_4^-$  and  $\text{AlCl}_4^-$  the ideal  $T_d$  symmetry ( $\alpha$ -angle equal to  $109.5^\circ$ ) is observed certainly.

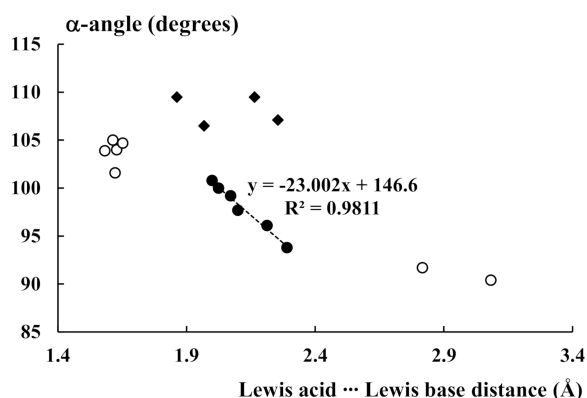


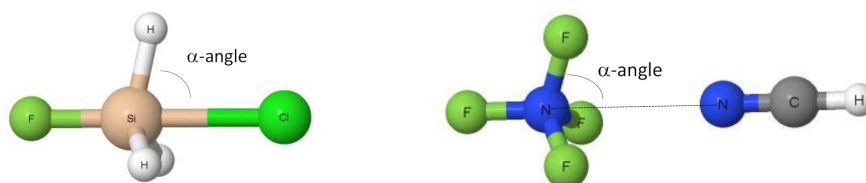
**Figure 6.** The dependence between the Lewis acid...Lewis base distance,  $T \dots B$ , (Å) and the  $\alpha$ -parameter (see Scheme 1) in A-T...B triel bonds (T-triel centre). Black and white circles correspond to the neutral complexes, aluminium and boron species, respectively. Squares correspond to anion complexes.

Thus one can see that the relationship presented in Figure 6 may be treated as the reaction path for the process of the change of trigonal and planar configuration into the tetrahedral structure; few complexes linked by the triel bond are stable structures characterised by large dissociation energies. It is interesting that these boron adducts characterised by the structures close to tetrahedral ones may further interact with the electron rich species according to the  $S_N2$  reaction mechanism.

The corresponding studies related to this topic appear from time to time, for example the reactions of borine carbonyl with trimethylamine and triethylamine were analysed experimentally early [92,93], or in more recent study, the  $S_N2$  reaction for the  $Cl^- \cdots CH_3Cl$  and  $NH_3 \cdots H_3BNH_3$  complexes were analysed theoretically [94], the latter one concerns the tetrahedral structure of boron.

## 6. Tetrel Bonds and the $S_N2$ Reaction

The tetrel bond is an interaction between the tetrel centre (14th group element) of the Lewis acid unit and the electron rich region of the moiety playing a role of the Lewis base [41,42,95–98]. The tetrel centre region that is responsible for the acidic (electron accepting) properties is classified as the  $\sigma$ -hole [95] but there are also cases of the tetrel centres that possess  $\pi$ -hole regions [98]. If the tetrel centre interacts with the Lewis base through the  $\sigma$ -hole thus the corresponding tetrel bond is often a preliminary stage of the  $S_N2$  reaction [97]. The tetrel bond as a type of the  $\sigma$ -hole bond leads to the geometrical changes of interacting units that the complex structure is close to the trigonal bipyramid, especially in a case of strong interactions [97]. Scheme 2 presents an example of the species connected by the  $\sigma$ -hole tetrel bond. It is the  $SiFH_3 \cdots Cl^-$  complex with the  $Si \cdots Cl$  intermolecular link and the  $SiH_3$  group in the central part of the complex that tends to the planarity. The latter situation is similar to those observed for transition states of  $S_N2$  reactions. Hence the similar parameter to that one discussed earlier here for the triel bonds (Scheme 1) may be introduced for tetrel  $\sigma$ -hole bonds. It is the  $\alpha$ -angle (Scheme 2) between the tetrel $\cdots$ Lewis base link and one of bonds of the tetrel species. For the example shown in Scheme 2 it is the angle between  $Si \cdots Cl$  line and the  $Si-H$  bond. For very strong interactions this angle is equal to  $90^\circ$  or nearly so. On the contrary, for extremely weak interactions that do not disturb the geometry of the Lewis acid unit the  $\alpha$ -angle should be equal to  $\sim 70.5^\circ$  that corresponds to the ideal tetrahedral structure of the tetrel species that is not perturbed by external forces.



**Scheme 2.** The  $SiFH_3 \cdots Cl^-$  and  $NF_4^+ \cdots NCH$  complexes linked by the tetrel bond and pnictogen bond, respectively.

This is interesting that similar characteristics are often observed for the charge assisted pnictogen species, which interact with the Lewis base units [99]. The complexes of  $ZH_4^+$ ,  $ZF_4^+$  and  $ZFH_3^+$  cations ( $Z = N, P, As$ ) were analysed theoretically and the  $Z \cdots$ Lewis base intermolecular links were observed [99] that may be classified as the type of  $\sigma$ -hole bonds, i.e., pnictogen bonds. These charge assisted pnictogen bonds also lead to the structural changes similar to those occurring for tetrel bonds, and they may be also classified as the preliminary stages of the  $S_N2$  reactions [99]. Scheme 2 presents the  $NF_4^+ \cdots NCH$  complex connected by the  $N \cdots N$  pnictogen bond. One of the nitrogen centres plays here a role of the electron acceptor while another N-centre is the electron donor. This is a very similar situation to that one occurring for the  $\sigma$ -hole tetrel bonds discussed here (see the same Scheme 2 with an example of the tetrel bonded complex).

Figure 7 presents the relationships between the tetrel/pnictogen centre $\cdots$ Lewis base centre distance and the  $\alpha$ -angle. Two sub-samples of complexes of tetrel species and one sub-sample of pnictogen species complexes are presented here. These geometrical results were taken from earlier studies [97,99] where the MP2/aug-cc-pVTZ calculations were performed on complexes presented in this figure. Let us describe the sub-samples presented in Figure 7. For that one with units linked by tetrel bond, the  $ZH_4$ ,  $ZFH_3$  and  $ZF_4$  ( $Z = C, Si, Ge$ ) species interact with the HCN and LiCN acting as Lewis bases (nitrogen atom is the Lewis base centre here). For the complexes with negatively charge assisted tetrel bonds the same Lewis acid units as for the former sub-sample interact with chloride anion. And for complexes

linked by the pnictogen bond the  $ZH_4^+$ ,  $ZFH_3^+$  and  $ZF_4^+$  species ( $Z = N, P$  and  $As$ ) interact with HCN and LiCN through the  $Z$  and nitrogen centres.

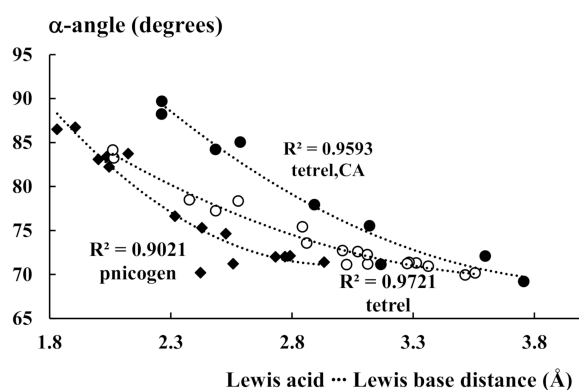


**Figure 7.** The dependence between the Lewis acid...Lewis base distance,  $Z\cdots B$ , (Å) and the  $\alpha$ -parameter (see Scheme 2) in A-Z...B tetrel and pnictogen bonds (Z-tetrel or pnictogen centre). Black and white circles correspond to the tetrel complexes linked by charge assisted tetrel bonds and neutral tetrel bonds, respectively. Squares correspond to complexes linked by the pnictogen bond.

Figure 7 shows that for shorter Lewis acid-base distances corresponding to stronger interactions, the  $\alpha$ -parameter (Scheme 2) tends to  $90^\circ$ . It means that the central part of the complex becomes to be planar as it is observed for the transition state of the  $S_N2$  reaction. The second order polynomial dependences between the distance and the  $\alpha$ -angle are observed here with high values of the correlation coefficients. These dependencies may be treated as the corresponding reaction paths of the above-mentioned  $S_N2$  reactions. This is very interesting that the pnictogen and tetrel  $\sigma$ -bonds considered here (Figure 7) do not practically differ between themselves. For both interactions the Lewis acid units possess the tetrahedral structure, for both interactions, the complexation leads to the geometrical changes towards the structure of trigonal bipyramid. And finally, both interactions may be considered as the preliminary stages of the  $S_N2$  reactions.

One can also mention C-H...M (M designates metal) contacts that often play an important role in catalysis [100]. These interactions are usually classified as attractive ones and they are named as agostic interactions in terms of the Dewar-Chatt-Duncanson model [101,102]. However, the term anagostic interactions was introduced [103] for such contacts that are sterically enforced in square-planar transition metal  $d^8$  complexes to distinguish them from attractive agostic interactions. The orbital interaction schemes were presented by Scherer and co-workers for various types of the C-H...M interactions [104]; these are: the above-mentioned repulsive anagostic 3c-4e interaction being the contact between hydric hydrogen and the filled M- $dz^2$  orbital, the attractive 3c-4e hydrogen bond being the interaction between the protic H-atom and the filled M- $dz^2$  orbital, preagostic attractive 3c-2e interaction ( $\pi$ -back donation) and the  $\sigma$ -agostic 3c-2e attractive interaction (hydric hydrogen–empty M- $dz^2$  orbital). On the other hand, in another study it was justified that the formation of numerous C-H...M structures is mainly driven by the dispersion forces thus the models based on the orbital-orbital interactions schemes are not sufficient to describe the nature of these structures [105]. It seems that both explanations, the “orbital based” explanation as well as that one considering dispersion forces, are valid. For example, in one of recent studies on the C-H...Ni contacts in  $Ni^{II}$  planar isomers the occurrence of the covalent type charge delocalisation and of the London dispersion forces was justified [106]. The latter study is based on experimental results that are supported by theoretical analyses where various approaches were applied [106]. However, it is worth noting that these C-H...M interactions, regardless of the mechanism of their formation, lead to the metal centre coordination change. In the case of square-planar structures with two additional C-H...M contacts the metal structure tends to the octahedral one. Hence the agostic interaction may be considered as a preliminary stage of the process of structural reconstruction.

## 7. Summary

Different interactions are discussed in this article; the hydrogen bond and its special type—the dihydrogen bond, the pnictogen, and tetrel bonds as representatives of the  $\sigma$ -hole bond, and the triel bond as an example of the  $\pi$ -hole bond. These interactions may be treated as preliminary stages of various reactions and processes; the proton transfer, the release of the molecular hydrogen, or the  $S_N2$  reaction.

However, it is also very important that intra- and intermolecular connections lead to numerous structural changes of the interacting units. The triel planar and trigonal species interacting with Lewis bases tend to achieve the tetrahedral geometry. On the other hand the tetrahedral tetrel moieties as well as the tetrahedral pnictogen cations, both characterised by the lack of the lone electron pairs, tend to attain the structure of the trigonal bipyramid. It is worth to mention that different structural changes take place for different species of the same element, like in a case of the  $\sigma$ -hole bonds on one hand and in a case of the  $\pi$ -hole bonds on the other hand. In general, there is a variety of numerous structural changes accompanying the processes of complexation.

Finally it is worth noting here that other interactions not discussed here may initiate various chemical reactions, there is room for numerous future studies related to this topic. One of the most important topics to be discussed in next studies is the application of the structure-correlation method [12–14]. This method may be generalised as the analysis of geometrical changes during the chemical reactions. One can see that Figures 1 and 2 presented in this study express the changes following the proton transfer process, Figure 6 shows such changes related to the transformation of the trigonal planar system into the tetrahedral structure while Figure 7 shows the reaction paths of the  $S_N2$  reactions.

**Funding:** This research was funded by the Spanish Government MINECO/FEDER, grant number PID2019-109555GB-I00 and Eusko Jaurlaritza, grant number IT-1254-19.

**Acknowledgments:** Technical and human support provided by Informatikako Zerbitzu Orokora - Servicio General de Informática de la Universidad del País Vasco (SGI/IZO-SGIker UPV/EHU), Ministerio de Ciencia e Innovación (MICINN), Gobierno Vasco Eusko Jaurlaritza (GV/EJ), European Social Fund (ESF) is gratefully acknowledged.

**Conflicts of Interest:** The authors declare no conflict of interest.

## References

1. Jeffrey, G.A.; Saenger, W. *Hydrogen Bonding in Biological Structures*; Springer: Berlin, Germany, 1991.
2. Jeffrey, G.A. *An Introduction to Hydrogen Bonding*; Oxford University Press: New York, NY, USA, 1997.
3. *Intermolecular Interactions in Crystals: Fundamentals of Crystal Engineering*; Novoa, J.J. Ed.; The Royal Society of Chemistry: London, UK, 2018.
4. Politzer, P.; Murray, J.S. Halogen Bonding: An Interim Discussion. *Chem. Phys. Chem.* **2013**, *14*, 278–294. [[CrossRef](#)] [[PubMed](#)]
5. Lewis, G.N. *Valence and the Structure of Atoms and Molecules*; American Chemical Society Monograph Series; The Chemical Catalog Company, Inc.: New York, NY, USA, 1923; p. 146.
6. Rauk, A. *Orbital Interaction Theory of Organic Chemistry*, 2nd ed.; John Wiley & Sons, Inc.: New York, NY, USA, 2001; p. XIII.
7. Grabowski, S.J. Hydrogen Bond and Other Lewis acid–Lewis Base Interactions—Mechanisms of Formation. In *Practical Aspects of Computational Chemistry IV*; Leszczynski, J., Shukla, M.K., Eds.; Springer Science: New York, NY, USA, 2016; Chapter 9; pp. 245–278.
8. Weinhold, F.; Landis, C. *Valency and Bonding, a Natural Bond Orbital Donor—Acceptor Perspective*; Cambridge University Press: Cambridge, UK, 2005.
9. Grabowski, S.J. What is the Covalency of Hydrogen Bonding? *Chem. Rev.* **2011**, *11*, 2597–2625. [[CrossRef](#)] [[PubMed](#)]
10. Kaplan, I.G. *Intermolecular Interactions: Physical Picture, Computational Methods and Model Potentials*; John Wiley & Sons, Ltd.: Chichester, UK, 2006; p. 1.

11. Grabowski, S.J. Hydrogen bonds, and  $\sigma$ -hole and  $\pi$ -hole bonds—mechanisms protecting doublet and octet electron structures. *Phys. Chem. Chem. Phys.* **2017**, *19*, 29742–29759. [[CrossRef](#)] [[PubMed](#)]
12. Dunitz, J.D. *Analysis of the Structure of Organic Molecules*; Cornell University Press: Ithaca, NY, USA, 1979.
13. Bürgi, H.B. Stereochemistry and Reaction Paths as Determined from Crystal Structure Data—A Relationship between Structure and Energy. *Angew. Chem. Int. Ed.* **1975**, *14*, 460–473. [[CrossRef](#)]
14. Bürgi, H.B.; Dunitz, J.D. From Crystal Statics to chemical dynamics. *Acc. Chem. Res.* **1983**, *16*, 153–161. [[CrossRef](#)]
15. Bürgi, H.B.; Dunitz, J.D.; Shefter, E. Geometrical reaction coordinates. II. Nucleophilic addition to a carbonyl group. *J. Am. Chem. Soc.* **1973**, *95*, 5065–5067. [[CrossRef](#)]
16. Grabowski, S.J.; Krygowski, T.M. The proton transfer path for C=O . . . H-O systems modelled from crystal structure data. *Chem. Phys. Lett.* **1999**, *305*, 247–250. [[CrossRef](#)]
17. Groom, C.R.; Bruno, I.J.; Lightfoot, M.P.; Ward, S.C. The Cambridge structural database. *Acta Cryst.* **2016**, *B72*, 171–179. [[CrossRef](#)]
18. Wong, R.; Allen, F.H.; Willett, P. The scientific impact of the Cambridge Structural Database: A citation-based study. *J. Appl. Cryst.* **2010**, *43*, 811–824. [[CrossRef](#)]
19. Wilson, C.C. *Single Crystal Neutron Diffraction from Molecular Materials*; World Scientific Publishing Co. Pre. Ltd.: Singapore, 2000.
20. Luger, P. *Modern X-Ray Analysis on Single Crystals*, 2nd ed.; Walter de Gruyter: Berlin, Germany, 2014.
21. Brown, I.D. Bond valences—A simple structural model for inorganic chemistry. *Chem. Soc. Rev.* **1978**, *7*, 359–376. [[CrossRef](#)]
22. Pauling, L. Atomic radii and interatomic distances in metals. *J. Am. Chem. Soc.* **1947**, *69*, 542–553. [[CrossRef](#)]
23. Gilli, P.; Bertolasi, V.; Ferretti, V.; Gilli, G. Covalent nature of the strong homonuclear hydrogen-bond—study of the OH . . . O system by crystal-structure correlation methods. *J. Am. Chem. Soc.* **1994**, *116*, 909–915. [[CrossRef](#)]
24. Robertson, J.M.; Ubbelohde, A.R. Structure and thermal properties associated with some hydrogen bonds in crystals. I. The isotope effect. *Proc. R. Soc. Lond. Ser. A* **1939**, *170*, 222–240.
25. Benedict, H.; Limbach, H.-H.; Wehlan, M.; Fehlhammer, W.-P.; Golubev, N.S.; Janoschek, R. Solid State <sup>15</sup>N-NMR and Theoretical Studies on Primary and Secondary Geometric H/D Isotope Effects on Low-Barrier NHN-Hydrogen Bonds. *J. Am. Chem. Soc.* **1998**, *120*, 2939–2950. [[CrossRef](#)]
26. Limbach, H.-H.; Tolstoy, P.M.; Pérez-Hernández, N.; Guo, J.; Shenderovich, I.G.; Denisov, G.S. OHO hydrogen bond geometries and NMR chemical shifts: From equilibrium structures to geometric H/D isotopic effects, with applications for water, protonated water, and compresses ice. *Isr. J. Chem.* **2009**, *49*, 199–216. [[CrossRef](#)]
27. Benedict, H.; Shenderovich, I.G.; Malkina, O.L.; Malkin, V.G.; Denisov, G.S.; Golubev, N.S.; Limbach, H.-H. Nuclear Scalar Spin-Spin Couplings and Geometries of Hydrogen Bonds. *J. Am. Chem. Soc.* **2000**, *122*, 1979–1988. [[CrossRef](#)]
28. Shenderovich, I.G.; Tolstoy, P.M.; Golubev, N.S.; Smirnov, S.N.; Denisov, G.S.; Limbach, H.-H. Low-Temperature NMR Studies of the Structure and Dynamics of a Novel Series of Acid–Base Complexes of HF with Collidine Exhibiting Scalar Couplings across Hydrogen Bonds. *J. Am. Chem. Soc.* **2003**, *125*, 11710–11720. [[CrossRef](#)] [[PubMed](#)]
29. Grabowski, S.J. Hydrogen bonds and other interactions as a response to protect doublet/octet electron structure. *J. Mol. Model.* **2018**, *24*, 38. [[CrossRef](#)] [[PubMed](#)]
30. Kryachko, E.S. Neutral Blue-Shifting and Blue-Shifted Hydrogen Bonds. In *Hydrogen Bonding—New Insights*; Grabowski, S.J., Ed.; Springer: Berlin/Heidelberg, Germany, 2006; Chapter 8; pp. 293–336.
31. Bader, R.F.W. *Atoms in Molecules, a Quantum Theory*; Oxford University Press: Oxford, UK, 1990.
32. Matta, C.; Boyd, R.J. (Eds.) *Quantum Theory of Atoms in Molecules: From Solid State to DNA and Drug Design*; Wiley-VCH Verlag GmbH & Co. KGaA: Weinheim, Germany, 2007.
33. Cremer, D.; Kraka, E. A Description of the Chemical Bond in Terms of Local Properties of Electron Density and Energy. *Croat. Chem. Acta* **1984**, *57*, 1259–1281.
34. Jenkins, S.; Morrison, I. The chemical character of the intermolecular bonds of seven phases of ice as revealed by AB initio calculation of electron densities. *Chem. Phys. Lett.* **2000**, *317*, 97–102. [[CrossRef](#)]
35. Arnold, W.D.; Oldfield, E. The Chemical Nature of Hydrogen Bonding in Proteins via NMR: *J*-Couplings, Chemical Shifts, and AIM Theory. *J. Am. Chem. Soc.* **2000**, *122*, 12835–12841. [[CrossRef](#)]

36. Rozas, I.; Alkorta, I.; Elguero, J. Behavior of ylides containing N, O, and C atoms as hydrogen bond acceptors. *J. Am. Chem. Soc.* **2000**, *122*, 1154–11161. [[CrossRef](#)]
37. Grabowski, S.J.; Lipkowski, P. Characteristics of XH... $\pi$  Interactions: Ab Initio and QTAIM Studies. *J. Phys. Chem. A* **2011**, *115*, 4765–4773. [[CrossRef](#)] [[PubMed](#)]
38. Clark, T.; Hennemann, M.; Murray, J.S.; Politzer, P. Halogen bonding: The  $\sigma$ -hole. *J. Mol. Model.* **2007**, *13*, 291–296. [[CrossRef](#)] [[PubMed](#)]
39. Politzer, P.; Lane, P.; Concha, M.C.; Ma, Y.; Murray, J.S. An overview of halogen bonding. *J. Mol. Model.* **2007**, *13*, 305–311. [[CrossRef](#)]
40. Politzer, P.; Riley, K.E.; Bulat, F.A.; Murray, J.S. Perspectives on halogen bonding and other  $\sigma$ -hole interactions: Lex parsimoniae (Occam's Razor). *Comput. Theor. Chem.* **2012**, *998*, 2–8. [[CrossRef](#)]
41. Politzer, P.; Murray, J.S.; Clark, T. Halogen bonding: An electrostatically-driven highly directional noncovalent interaction. *Phys. Chem. Chem. Phys.* **2010**, *12*, 7748–7758. [[CrossRef](#)]
42. Politzer, P.; Murray, J.S.; Clark, T. Halogen bonding and other  $\sigma$ -hole interactions: A perspective. *Phys. Chem. Chem. Phys.* **2013**, *15*, 11178–11189. [[CrossRef](#)]
43. Grabowski, S.J. Boron and other triel Lewis acid centers: From hypovalency to hypervalency. *Chem. Phys. Chem.* **2014**, *15*, 2985–2993. [[CrossRef](#)]
44. Grabowski, S.J.  $\pi$ -hole bonds: Boron and aluminium Lewis acid centers. *Chem. Phys. Chem.* **2015**, *16*, 1470–1479. [[CrossRef](#)]
45. Scheiner, S. Detailed Comparison of the Pnictogen Bond with Chalcogen, Halogen, and Hydrogen Bonds. *Int. J. Quantum Chem.* **2013**, *113*, 1609–1620. [[CrossRef](#)]
46. Scheiner, S. The Pnictogen Bond: Its Relation to Hydrogen, Halogen, and Other Noncovalent Bonds. *Acc. Chem. Res.* **2013**, *46*, 280–288. [[CrossRef](#)] [[PubMed](#)]
47. Grabowski, S.J. Hydrogen and halogen bonds are ruled by the same mechanisms. *Phys. Chem. Chem. Phys.* **2013**, *15*, 7249–7259. [[CrossRef](#)] [[PubMed](#)]
48. Turunen, L.; Erdélyi, M. Halogen Bonds and Halonium Ions. *Chem. Soc. Rev.* **2020**, *49*, 2688–2700. [[CrossRef](#)]
49. Holl, M.G.; Pitts, C.R.; Lectka, T. Quest for a Symmetric [C–F–C]<sup>+</sup> Fluoronium Ion in Solution: A Winding Path to Ultimate Success. *Acc. Chem. Res.* **2020**, *53*, 265–275. [[CrossRef](#)]
50. Struble, M.D.; Scerba, M.T.; Siegler, M.; Lectka, T. Evidence for a Symmetrical Fluoronium Ion in Solution. *Science* **2013**, *340*, 57–60. [[CrossRef](#)]
51. Hennecke, U. Revealing the Positive Side of Fluorine. *Science* **2013**, *340*, 41–42. [[CrossRef](#)]
52. Reiersølmoen, A.C.; Battaglia, S.; Øien-Ødegaard, S.; Gupta, A.K.; Fiksdahl, A.; Lindh, R.; Erdélyi, M. Symmetry of three-center, four-electron bonds. *Chem. Sci.* **2020**, *11*, 7979–7990. [[CrossRef](#)]
53. Bedin, N.; Karim, A.; Reitti, M.; Carlsson, A.C.C.; Topić, F.; Cetina, M.; Pan, F.; Havel, V.; Al-Ameri, F.; Sindelar, V.; et al. Counterion influence on the N–I–N halogen bond. *Chem. Sci.* **2015**, *6*, 3746–3756. [[CrossRef](#)]
54. Villarreal-Salinas, B.E.; Schlemper, E.O. Crystal structure of a salt of the pyridinium-pyridine ion by X-ray and neutron diffraction. *J. Cryst. Mol. Struct.* **1978**, *8*, 217–237. [[CrossRef](#)]
55. Ward, J.S.; Fiorini, G.; Frontera, A.; Rissanen, K. Asymmetric [N–I–N]<sup>+</sup> halonium complexes. *Chem. Commun.* **2020**, *56*, 8428–8431. [[CrossRef](#)]
56. Zundel, G. *Series of Ten Lectures On: Proton Polarizability of Hydrogen Bonds and Proton Transfer Processes, Their Role in Electrochemistry and Biology*; Institut für Physikalische Chemie der Universität München: München, Germany, 1997.
57. Kong, S.; Borissova, A.O.; Lesnichin, S.B.; Hartl, M.; Daemen, L.L.; Eckert, J.; Antipin, M.Y.; Shenderovich, I.G. Geometry and Spectral Properties of the Protonated Homodimer of Pyridine in the Liquid and Solid States. A Combined NMR, X-ray Diffraction and Inelastic Neutron Scattering Study. *J. Phys. Chem. A* **2011**, *115*, 8041–8048. [[CrossRef](#)]
58. Gurinov, A.A.; Lesnichin, S.B.; Limbach, H.-H.; Shenderovich, I.G. How Short is the Strongest Hydrogen Bond in the Proton-Bound Homodimers of Pyridine Derivatives? *J. Phys. Chem. A* **2014**, *118*, 10804–10812. [[CrossRef](#)] [[PubMed](#)]
59. Wenthold, P.G.; Squires, R.R. Bond Dissociation Energies of F<sub>2</sub><sup>−</sup> and HF<sub>2</sub><sup>−</sup>. A Gas-Phase Experimental and G2 Theoretical Study. *J. Phys. Chem.* **1995**, *99*, 2002–2005. [[CrossRef](#)]
60. Grabowski, S.J. [FHF]<sup>−</sup>-The Strongest Hydrogen Bond under the Influence of External Interactions. *Crystals* **2016**, *6*, 3. [[CrossRef](#)]



61. Grabowski, S.J.; Ugalde, J.M. High-level ab initio calculations on low barrier hydrogen bonds and proton bound homodimers. *Chem. Phys. Lett.* **2010**, *493*, 37–44. [[CrossRef](#)]
62. Sobczyk, L.; Grabowski, S.J.; Krygowski, T.M. Interrelation between H-Bond and Pi-Electron Delocalization. *Chem. Rev.* **2005**, *105*, 3513–3560. [[CrossRef](#)]
63. Richardson, T.B.; de Gala, S.; Crabtree, R.H. Unconventional Hydrogen Bonds: Intermolecular B-H ... H-N Interactions. *J. Am. Chem. Soc.* **1995**, *117*, 12875–12876. [[CrossRef](#)]
64. Epstein, L.M.; Shubina, E.S. New types of hydrogen bonding in organometallic chemistry. *Coord. Chem. Rev.* **2002**, *231*, 165–181. [[CrossRef](#)]
65. Bakmutov, V.I. *Dihydrogen Bonds, Principles, Experiments, and Applications*; John Wiley & Sons: Hoboken, NJ, USA, 2008.
66. Kubas, G.J. *Metal Dihydrogen and  $\sigma$ -Bond Complexes—Structure, Theory, and Reactivity*; Kluwer Academic/Plenum Publishers: New York, NY, USA, 2001.
67. Crabtree, R.H. *The Organometallic Chemistry of the Transition Metals*; John Wiley & Sons, Inc.: Hoboken, NJ, USA, 2005.
68. Rozas, I.; Alkorta, I.; Elguero, J. Field effects on dihydrogen bonded systems. *Chem. Phys. Lett.* **1997**, *275*, 423–428. [[CrossRef](#)]
69. Custelcean, R.; Jackson, J.E. Topochemical Control of Covalent Bond Formation by Dihydrogen Bonding. *J. Am. Chem. Soc.* **1998**, *120*, 12935–12941. [[CrossRef](#)]
70. Custelcean, R.; Jackson, J.E. Topochemical Dihydrogen to Covalent Bonding Transformation in  $\text{LiBH}_4 \cdot \text{TEA}$ : A Mechanistic Study. *J. Am. Chem. Soc.* **2000**, *122*, 5251–5257. [[CrossRef](#)]
71. Marincean, S.; Jackson, J.E. Quest for IR-pumped reactions in dihydrogen-bonded complexes. *J. Phys. Chem. A* **2004**, *108*, 5521–5526. [[CrossRef](#)]
72. Grabowski, S.J.; Ruipérez, F. Dihydrogen bond interactions as a result of  $\text{H}_2$  cleavage at Cu, Ag and Au centres. *Phys. Chem. Chem. Phys.* **2016**, *18*, 12810–12818. [[CrossRef](#)]
73. Grabowski, S.J. The Nature of Triel Bonds, a Case of B and Al Centres Bonded with Electron Rich Sites. *Molecules* **2020**, *25*, 2703. [[CrossRef](#)]
74. Brinck, T.; Murray, J.S.; Politzer, P. A computational analysis of the bonding in boron trifluoride and boron trichloride and their complexes with ammonia. *Inorg. Chem.* **1993**, *32*, 2622–2625. [[CrossRef](#)]
75. Bessac, F.; Frenking, G. Why Is  $\text{BCl}_3$  a Stronger Lewis Acid with Respect to String Bases than  $\text{BF}_3$ ? *Inorg. Chem.* **2003**, *42*, 7990–7994. [[CrossRef](#)]
76. Jonas, V.; Frenking, G.; Reetz, M.T. Comparative Theoretical Study of Lewis Acid-Base Complexes of  $\text{BH}_3$ ,  $\text{BF}_3$ ,  $\text{BCl}_3$ ,  $\text{AlCl}_3$ , and  $\text{SO}_2$ . *J. Am. Chem. Soc.* **1994**, *116*, 8741–8753. [[CrossRef](#)]
77. Van der Veken, B.J.; Sluyts, E.J. Reversed Lewis Acidity of Mixed Boron Halides: An Infrared Study of the Van der Waals Complexes of  $\text{BF}_x\text{Cl}_y$  with  $\text{CH}_3\text{F}$  in Cryosolution. *J. Am. Chem. Soc.* **1997**, *119*, 11516–11522. [[CrossRef](#)]
78. Phillips, J.A. Structural and energetic properties of nitrile- $\text{BX}_3$  complexes: Substituent effects and their impact on condensed-phase sensitivity. *Theor. Chem. Acc.* **2017**, *136*, 16. [[CrossRef](#)]
79. Giesen, D.J.; Phillips, J.A. Structure, Bonding, and Vibrational Frequencies of  $\text{CH}_3\text{CN-BF}_3$ : New Insight into Medium Effects and the Discrepancy between the Experimental and Theoretical Geometries. *J. Phys. Chem. A* **2003**, *107*, 4009–4018. [[CrossRef](#)]
80. Phillips, J.A.; Cramer, C.J. B-N Distance Potential of  $\text{CH}_3\text{CN-BF}_3$  Revisited: Resolving the Experiment-Theory Structure Discrepancy and Modeling the Effects of Low-Dielectric Environments. *J. Phys. Chem. B* **2007**, *111*, 1408–1415. [[CrossRef](#)] [[PubMed](#)]
81. Wrass, J.P.; Sadowsky, D.; Bloomgren, K.M.; Cramer, C.J.; Phillips, J.A. Quantum chemical and matrix-IR characterization of  $\text{CH}_3\text{CN-BCl}_3$ : A complex with two distinct minima along the B-N bond potential. *Phys. Chem. Chem. Phys.* **2014**, *16*, 16480–16491. [[CrossRef](#)] [[PubMed](#)]
82. Helminiak, H.M.; Knauf, R.R.; Danforth, S.J.; Phillips, J.A. Structural and Energetic Properties of Acetonitrile-Group IV (A & B) Halide Complexes. *J. Phys. Chem. A* **2014**, *118*, 4266–4277.
83. Grabowski, S.J. Two Faces of Triel Bonds in Boron Trihalide Complexes. *J. Comput. Chem.* **2018**, *39*, 472–480. [[CrossRef](#)]
84. Grabowski, S.J. Triel bond and coordination of triel centres—Comparison with hydrogen bond interaction. *Coord. Chem. Rev.* **2020**, *407*, 213171. [[CrossRef](#)]

85. Fau, S.; Frenking, G. Theoretical investigation of the weakly bonded donor—Acceptor complexes  $X_3B-H_2$ ,  $X_3B-C_2H_4$ , and  $X_3B-C_2H_2$  ( $X = H, F, Cl$ ). *Mol. Phys.* **1999**, *96*, 519–527.
86. Grabowski, S.J. Triel Bonds,  $\pi$ -Hole- $\pi$ -Electrons Interactions in Complexes of Boron and Aluminium Trihalides and Trihydrides with Acetylene and Ethylene. *Molecules* **2015**, *20*, 11297–11316. [[CrossRef](#)]
87. Grabowski, S.J. Triel bonds-complexes of boron and aluminum trihalides and trihydrides with benzene. *Struct. Chem.* **2017**, *28*, 1163–1171. [[CrossRef](#)]
88. Grabowski, S.J. Molecular Hydrogen as a Lewis Base in Hydrogen Bonds and Other Interactions. *Molecules* **2020**, *25*, 3294. [[CrossRef](#)]
89. Grabowski, S.J. Bifurcated Triel Bonds—Hydrides and Halides of 1,2-Bis(Dichloroboryl)Benzene and 1,8-Bis(Dichloroboryl)Naphthalene. *Crystals* **2019**, *9*, 503. [[CrossRef](#)]
90. Etter, M.C. Encoding and Decoding Hydrogen-Bond Patterns of Organic Compounds. *Acc. Chem. Res.* **1990**, *23*, 120–126. [[CrossRef](#)]
91. Grabowski, S.J. Hydrogen bonds with  $BF_4^-$  anion as a proton acceptor. *Crystals* **2020**, *10*, 460. [[CrossRef](#)]
92. Grotewold, J.; Lisi, E.A.; Villa, A.E. Reactions of Co-ordinated Boron Compounds in the Gas Phase. Part I. Borine Carbonyl and Trimethylamine. *J. Chem. Soc. A* **1966**, 1034–1037. [[CrossRef](#)]
93. Grotewold, J.; Lisi, E.A.; Villa, A.E. Reactions of Co-ordinated Boron Compounds in the Gas Phase. Part II. Triethylamine as Scavenger of Borine. *J. Chem. Soc. A* **1966**, 1038–1041. [[CrossRef](#)]
94. Yang, S.-Y.; Fleurat-Lessard, P.; Hristov, I.; Ziegler, T. Free Energy Profiles for the Identity  $S_N2$  Reactions  $Cl^- + CH_3Cl$  and  $NH_3 + H_3BNH_3$ : A Constraint Ab Initio Molecular Dynamics Study. *J. Phys. Chem. A* **2004**, *108*, 9461–9468. [[CrossRef](#)]
95. Bundhun, A.; Ramasami, P.; Murray, J.S.; Politzer, P. Trends in  $\sigma$ -hole Strengths and Interactions of  $F_3MX$  Molecules ( $M = C, Si, Ge$  and  $X = F, Cl, Br, I$ ). *J. Mol. Model.* **2013**, *19*, 2739–2746. [[CrossRef](#)]
96. Bauzá, A.; Mooibroek, T.J.; Frontera, A. Tetrel-Bonding Interaction: Rediscovered Supramolecular Force? *Angew. Chem. Int. Ed.* **2013**, *52*, 12317–12321. [[CrossRef](#)]
97. Grabowski, S.J. Tetrel bond- $\sigma$ -hole bond as a preliminary stage of the  $S_N2$  reaction. *Phys. Chem. Chem. Phys.* **2014**, *16*, 1824–1834. [[CrossRef](#)]
98. Zierkiewicz, W.; Michalczyk, M.; Scheiner, S. Comparison between Tetrel Bonded Complexes Stabilized by  $\sigma$  and  $\pi$  Hole Interactions. *Molecules* **2018**, *23*, 1416. [[CrossRef](#)]
99. Grabowski, S.J.  $\sigma$ -Hole Bond versus Hydrogen Bond: From Tetravalent to Pentavalent, N, P and As Atoms. *Chem. Eur. J.* **2013**, *19*, 14600–14611. [[CrossRef](#)] [[PubMed](#)]
100. Scherer, W.; McGrady, G.S. Agostic Interactions in  $d^0$  Metal Alkyl Complexes. *Angew. Chem. Int. Ed.* **2004**, *43*, 1782–1806. [[CrossRef](#)] [[PubMed](#)]
101. Dewar, M.J.S. A review of the  $\pi$ -complex theory. *Bull. Soc. Chim. Fr.* **1951**, *18*, C71–C79.
102. Chatt, J.; Duncanson, L.A. Olefin Co-ordination Compounds. Part III. Infra-red Spectra and Structure: Attempted Preparation of Acetylene Complexes. *J. Chem. Soc.* **1953**, 2939–2947. [[CrossRef](#)]
103. Sundquist, W.I.; Bancroft, D.P.; Lippard, S.J. Synthesis, characterization, and biological activity of cis-diammineplatinum(II) complexes of the DNA intercalators 9-aminoacridine and chloroquine. *J. Am. Chem. Soc.* **1990**, *112*, 1590–1596. [[CrossRef](#)]
104. Scherer, W.; Dunbar, A.C.; Barquera-Lozada, J.E.; Schmitz, D.; Eickerling, G.; Kratzert, D.; Stalke, D.; Lanza, A.; Macchi, P.; Casati, N.P.M.; et al. Anagostic Interactions under Pressure: Attractive or Repulsive? *Angew. Chem. Int. Ed.* **2015**, *54*, 2505–2509. [[CrossRef](#)]
105. Lu, Q.; Neese, F.; Bistoni, G. Formation of Agostic Structures Driven by London Dispersion. *Angew. Chem. Int. Ed.* **2018**, *57*, 4760–4764. [[CrossRef](#)]
106. Mitoraj, M.P.; Babashkina, M.G.; Robeyns, K.; Sagan, F.; Szczepanik, D.W.; Seregina, Y.V.; Garcia, Y.; Safin, D.A. Chameleon-like Nature of Anagostic Interactions and Its Impact on Metalloaromaticity in Square-Planar Nickel Complexes. *Organometallics* **2019**, *38*, 1973–1981. [[CrossRef](#)]

